Electronic Supplementary Information for

Light-Activated Controlled Release of Camptothecin by Engineering Porous Materials: The *Ship in a Bottle* Concept in Drug Delivery

Eva Rivero-Buceta,[a] Mirela E. Encheva,[b] Bradley Cech,[c] Eduardo Fernandez,[b] Germán Sastre,[a] Christopher C. Landry,[c,] and Pablo Botella, [a,]**

[a] Instituto de Tecnología Química, Universitat Politècnica de València-Consejo Superior de Investigaciones Científicas, Avenida de los Naranjos s/n, 46022 Valencia, Spain

[b] Institute of Bioengineering, Universidad Miguel Hernández, Elche, Spain and Centre for Network Biomedical Research (CIBER-BBN), Avenida de la Universidad s/n 03202 Elche, Spain

[c] Department of Chemistry, University of Vermont, 82 University Place, Burlington, VT 05405, USA

*To whom correspondence should be addressed. E-mail: pbotella@itq.upv.es; Christopher.Landry@uvm.edu

1. Reagents and cells

1.1. Reagents

Camptothecin was obtained from Fluorochem. Pluronic F-127, triethylamine (TEA), 4-dimetilaminopiridine (DMAP), N,N′-Diisopropylcarbodiimide (DIC), N-(tert-butoxycarbonyl)glycine, 1,3,5-trimethylbenzene, Dimethyl Sulfoxide (DMSO) and anhydrous solvents were purchased by Sigma-Aldrich. Fluorocarbon surfactant FC-4 was purchased by Yick-Vic Chemicals & Pharmaceuticals (HK). Tetraethyl orthosilicate (TEOS) was supplied from Merck Millipore. Azobenzene-4,4'-dicarbonyl dichloride was purchased by TCI Europe. HPLC grade solvents were supplied by Scharlab. Water was deionized to 18.2 MΩ cm^{-1} using a milliQ pack system.

1.2. Cells

Human HeLa cervix carcinoma, human U251 glioblastoma and human SH-SY5Y neuroblastoma cell lines were obtained from American Type Cell Culture (ATCC, Rockfield, MD) and cultured in Dulbecco's Modified Eagle Medium (DMEM) supplemented with 10 % fetal bovine serum (FBS, from Lonza, Verviers, Belgium) and 1 % penicillin and streptomycin (from Gibco) under a humidified atmosphere (5 % CO_2) at 37 °C.

2. Molecular Dynamics

2.1. Methodology.

Azobenzene is known to be more stable in the *trans* isomer, but irradiation with UV light (350 nm) leads to isomerisation to the *cis* isomer. Two mechanisms have been proposed,[1] either through an inversion of the C-N=N angle (from the equilibrium ~120º to ~240º) or a rotation of the C-N=N-C dihedral from 180º to the equilibrium angle in the *cis* conformation, close to 0º. In both cases, the adsorbed light excites an electron from the S_0 ground state (whose minimum corresponds to the *trans* configuration) to the excited S_1 state. In the inversion mechanism, the S_1 surface has a minimum C-N=N angle of ~240º (*cis* conformation) and, after a fast relaxation, the molecule remains in the *cis* conformation until irradiation stops, by returning the electron to the S_0 state where the minimum is at 120º (*trans* conformation). In the rotation mechanism, the S_1 excited state shows a minimum at a dihedral C-N=N-C angle of ~90º, showing a conical intersection with the S_0 state at a point leading to relaxation of the molecule along S_0 in either of the two relative minima, 180º (*trans*) or 0º (*cis*). When the molecule is in the *cis* configuration, the molecular vibrations/rotations lead to a further relaxation to the absolute minimum (*trans*). Thus, according to this mechanism, during irradiation the conformation is intermediate (90º) between *cis* and *trans*; after irradiation, the molecule can relax to *cis* (where it will remain for a short time) or *trans*, the more stable conformation.

This process can be simulated using atomic force fields by using different strategies.[2,3]

In our study we have chosen to employ the force field by Oie et al.[4] in order to model the intramolecular terms of the azobenzene molecules. This force field is general to an enormous variety of organic molecules and employs simple functions for the two-, three- and four-body bonding terms (equation SE1).

$$V_{azobenz} = k_{bond} \cdot (r - r_0)^2 + k_{angle} \cdot (\theta - \theta_0)^2 + k_{dihedral} \cdot (1 \pm cos(n \cdot \phi)) + V_{coul} + V_{vdW} \qquad (SE1)$$

Since this is, as usual, a force field that describes the ground state, it can not stabilise the *cis* conformation, and to do that we have modified the constant of the corresponding equation SE2:

$$E_{torsion}(C - N = N - C) = k_{\phi} \cdot (1 - cos(2 \cdot \phi)) \qquad (SE2)$$

Where for the *trans* conformation we have used the default value of 20.9 kJ/mol whilst for the *cis* we have used the value of 83.7 kJ/mol taken from ref. 1. With the latter value, and starting from a *cis* (ϕ=0º) configuration, which is a relative minimum in eq. 2, the molecule does not isomerise to *trans* at the temperature (298 K) of the simulations. This is our approximation to the behaviour of the molecule while it is irradiated in order to favour the *cis* conformation.

Van der Waals interaction between atom pairs in the system, excluding bonded atoms and 1-3 bonded, have been approximated by a Lennard-Jones 12-6 potential according to the UFF (Universal Force-field) parameterisation. For hydrogen atoms a second set of parameters by Bureekaew et al.,[5] and employed in

previous work,[6] has also been tested, but our results indicate that the UFF, finally selected, reflects better the short range interactions in the azobenzene molecules.

DL_POLY 2.20[7] was used for the molecular dynamic simulations, which were carried out including full flexibility and periodic boundary conditions (cubic box of 50 Å containing one molecule) for all the atoms of the molecule. The temperature chosen is 298 K within the NVT ensemble. We employed the Verlet-leapfrog integration algorithm and the Evans thermostat, with a time step of 1 fs. Each run comprised an equilibration stage of 1×10^4 steps followed by the necessary production stage so as to ensure sufficiently good statistics for the analysis of 3×10^5 steps (300 ps). The cut-off for the non-bonding forces was set to 9 Å, and the Ewald summation was employed for the Coulombic with a precision parameter set to 10^{-4}. The configurations were saved every 10 time-steps (0.01 ps), giving a number of 30000, large enough to obtain good statistics and allowing a smooth visualisation of the dynamics.

2.2. Molecular dynamics simulation of CAABE compound

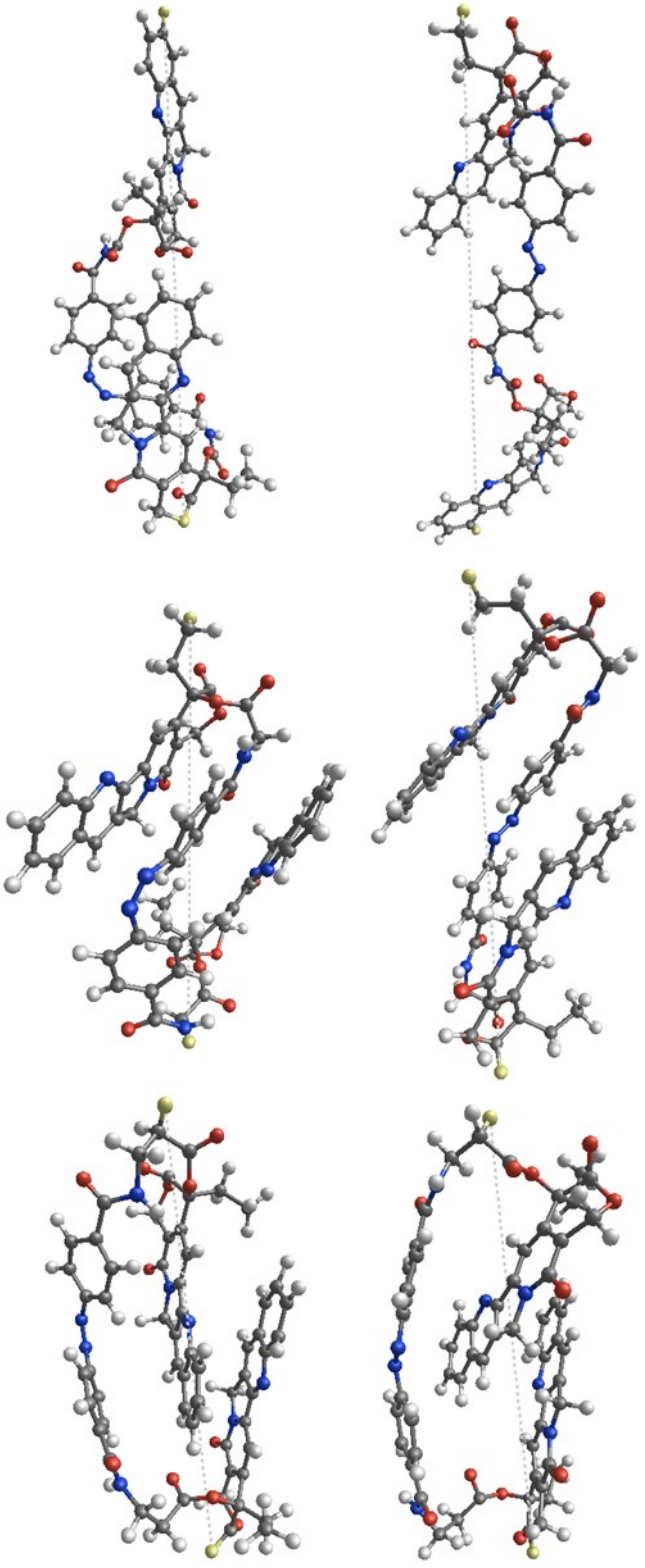

Fig. S1. Definition of maximum distance (molecular size, Å), dotted line, between pairs of atoms (highlighted in yellow) in the three (*n*=0,1,2) (top, middle, bottom) *cis/trans* (left, right) azobenzenes.

Additional information on the folding of *cis/trans*-CAABE isomers is also presented in molecular dynamics movies, as described below:

n	Isomer	movie
0	*cis*-CAABE	Video SV2-n=0 cis.mp4
0	*trans*-CAABE	Video SV3-n=0 trans.mp4
1	*cis*-CAABE	Video SV4-n=1 cis.mp4
1	*trans*-CAABE	Video SV5-n=1 trans.mp4
2	*cis*-CAABE	Video SV6-n=2 cis.mp4
2	*trans*-CAABE	Video SV7-n=2 trans.mp4

3. Preparation of CAABE

3.1. Synthesis of CAABE compound

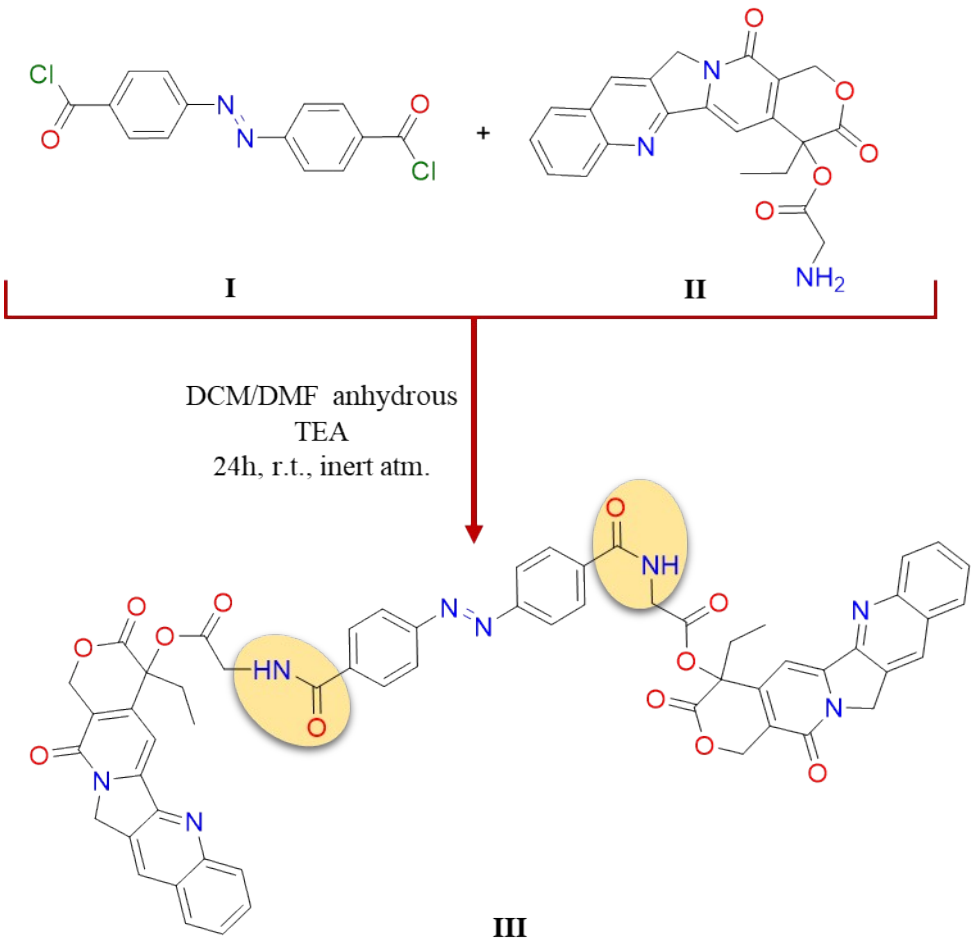

Fig. S2. Synthesis scheme of CAABE prodrug.

3.2. Characterization of CAABE

NMR spectra were recorded on a Bruker AV300 Ultrashield™ spectrometrer. ^{1}H NMR spectra were acquired at 300 MHz employing pulses of 15 µsec and a recycle time of 1 sec. Data for ^{1}H spectra are reported as follows: chemical shift, multiplicity (s = singlet, d = doublet, dd = doublet of doublet, t = triplet, dt = doublet of triplet, m = multiplet) and integration. To obtain ^{13}C spectra 9 µsec pulses at 75 MHz were applied with a recycle time of 2 seconds. Both ^{1}H and ^{13}C experiments were carried out using tetramethylsilane (TMS) as chemical shift reference. Two-dimensional correlation spectroscopy (2D-COSY) spectrum was acquired with 64 scans and 2 s relaxation delay. Two-dimensional heteronuclear single quantum coherence (2D-HSQC) spectrum was obtained with 96 scans, 1.15 s relaxation delay and a sweep width of 0 to 157 ppm. Exact mass values were obtained using a Quadrupole time-of-flight (Q-Tof) spectrometer (Xevo Qtof MS) coupled with a liquid chromatography system (Acquity UPLC Waters). The data was performed using a mobile phase consisting of solvent A (H_2O + 0.1% Formic Acid) and solvent B (CH_3CN + 0.1 % Formic acid) with a flow rate of 0.5 mL

min^{-1} (0-2 min 60% A/40% B; 3-8 min 50% A/50% B, 9 min 60% A/40% B). 10 µL of samples were injected and collected in the positive mode.

3.2.1 ^{1}H-NMR Spectra

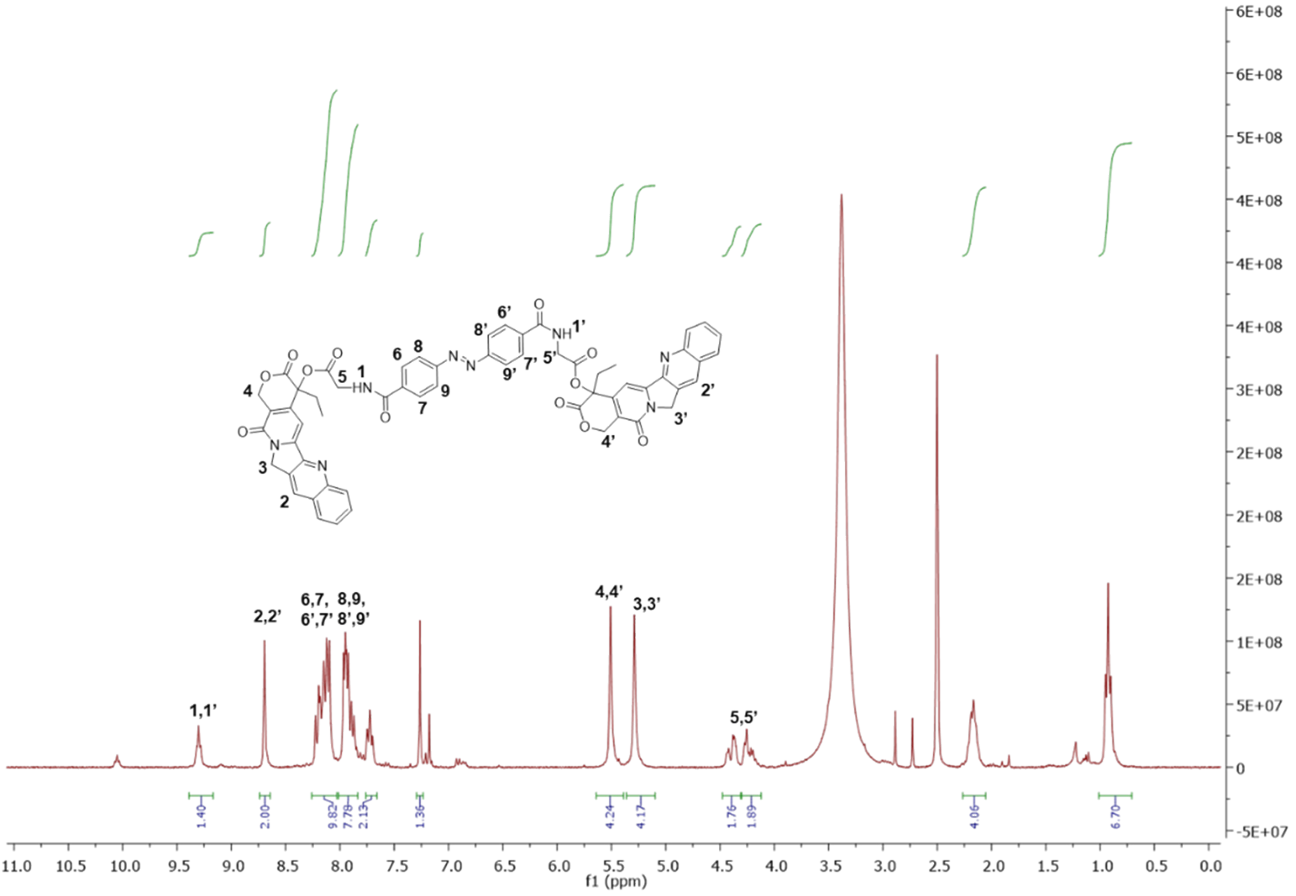

^{1}H-NMR (300 MHz, DMSO-d$_6$, δ_H): 0.93 (t, *J*=7.4 Hz, 6H), 2.18 (m, 4H), 4.14 - 4.47 (m, 4H), 5.30 (s, 4H), 5.51 (s, 4H), 7.27 (s, 2H), 7.75 (t, *J*=7.5 Hz, 2H), 7.94 (m, 6H. 4 azo H-meta hydrogen atoms), 8.16 (m, 8H. 4 azo H-ortho hydrogen atoms), 8.70 (s, 2H), 9.32 (t, *J*=5.8 Hz, 2H).

Fig. S3. ^{1}H-NMR spectrum of CAABE compound.

3.2.2. ^{13}C-NMR Spectra

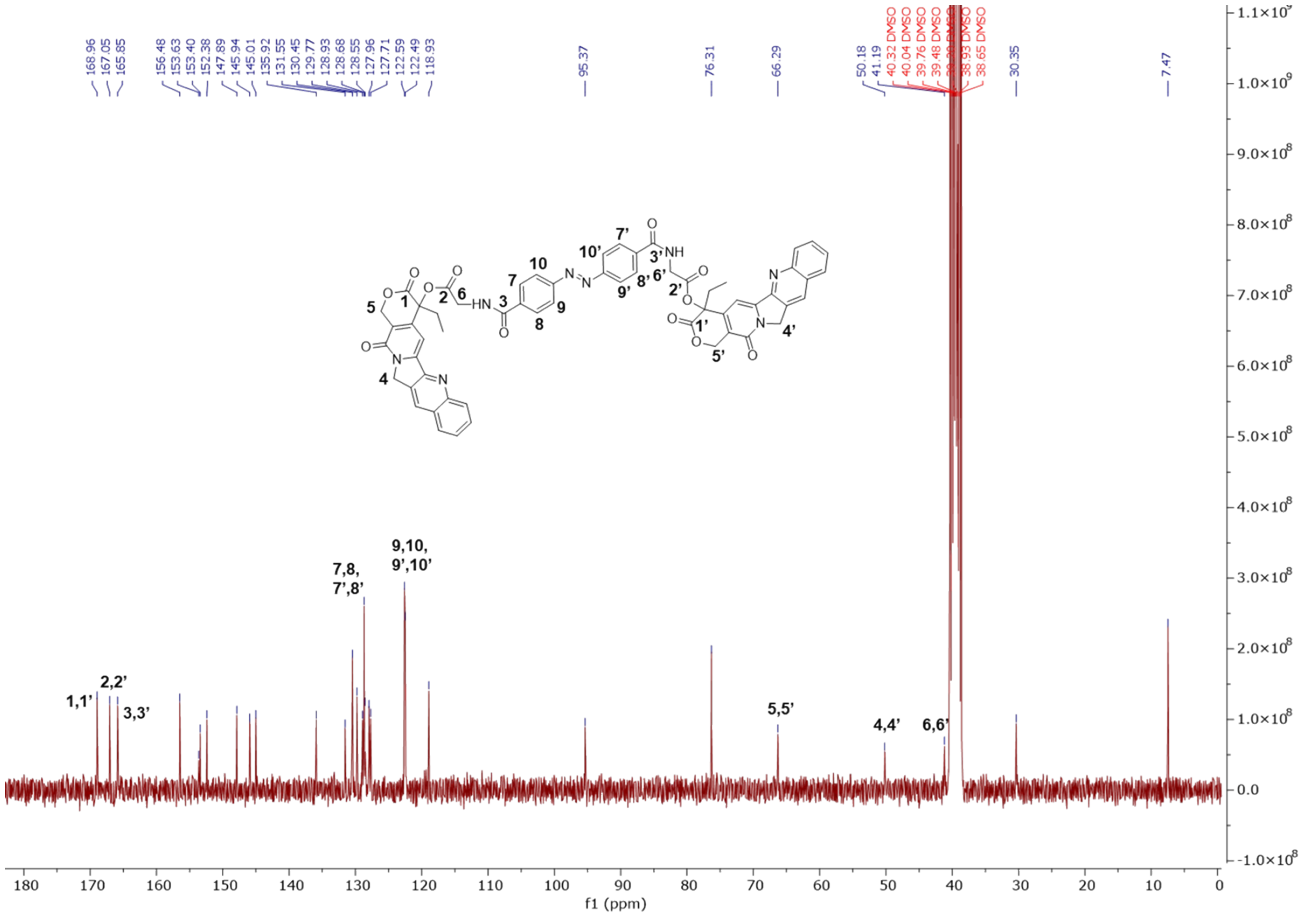

^{13}C-NMR (75 MHz, DMSO-d$_6$, δ_C): 7.47, 30.35, 41.19, 50.18, 66.29, 76.31, 95.37, 118.93, 122.49, 122.59, 127.71, 127.96, 128.55, 128.68, 128.93, 129.77, 130.45, 131.55, 135.92, 145.01, 145.94, 147.89, 152.38, 153.40, 153.63, 156.48, 165.85, 167.05, 168.96.

Fig. S4. ^{13}C-NMR spectrum of CAABE compound.

3.2.3. 2D-COSY NMR Spectra

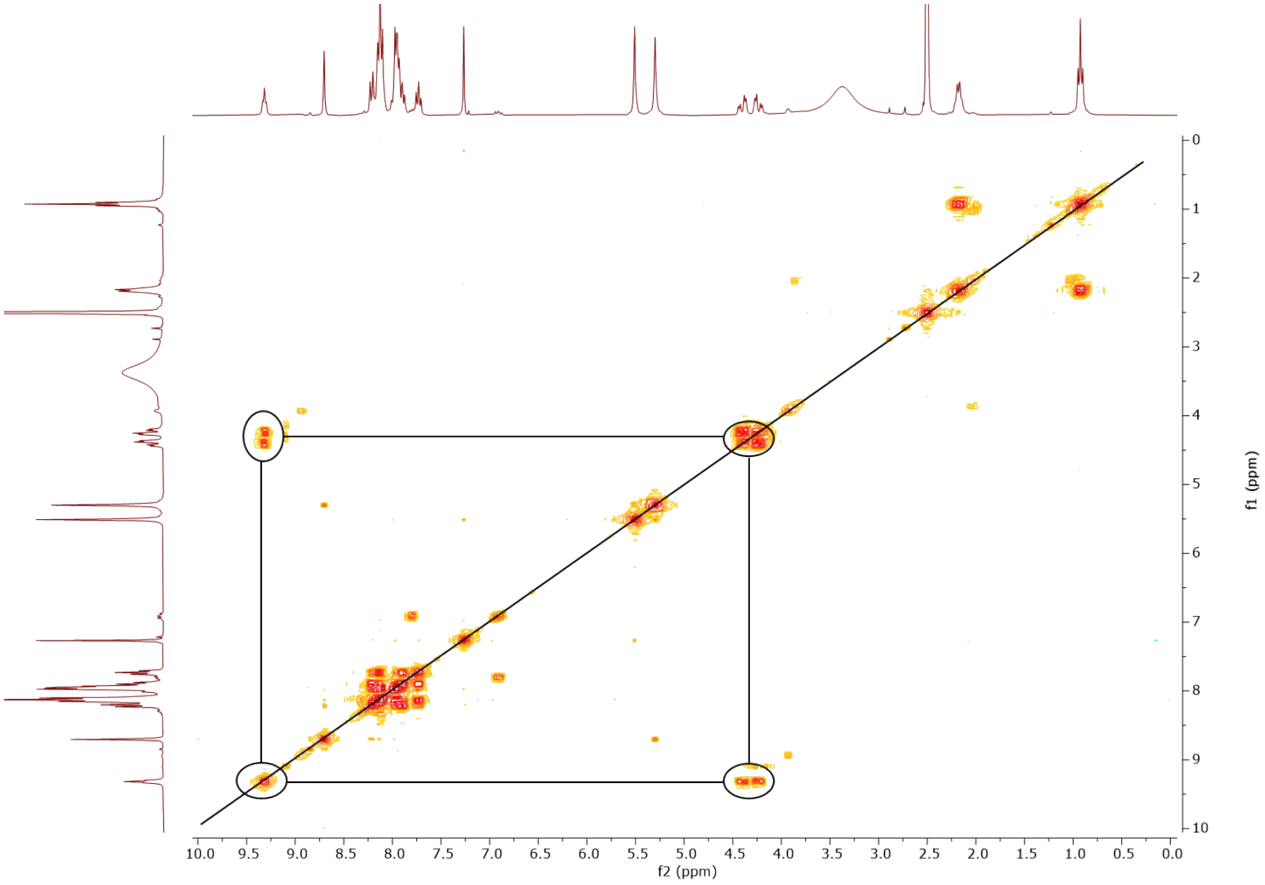

Fig. S5. 2D-COSY spectrum of CAABE compound. The correlation point between the proton of the amide group (9.32 ppm) and the methylene protons of the glycine moiety between 4.14 and 4.47 ppm is indicated in black.

3.2.4. 2D-HSQC NMR Spectra

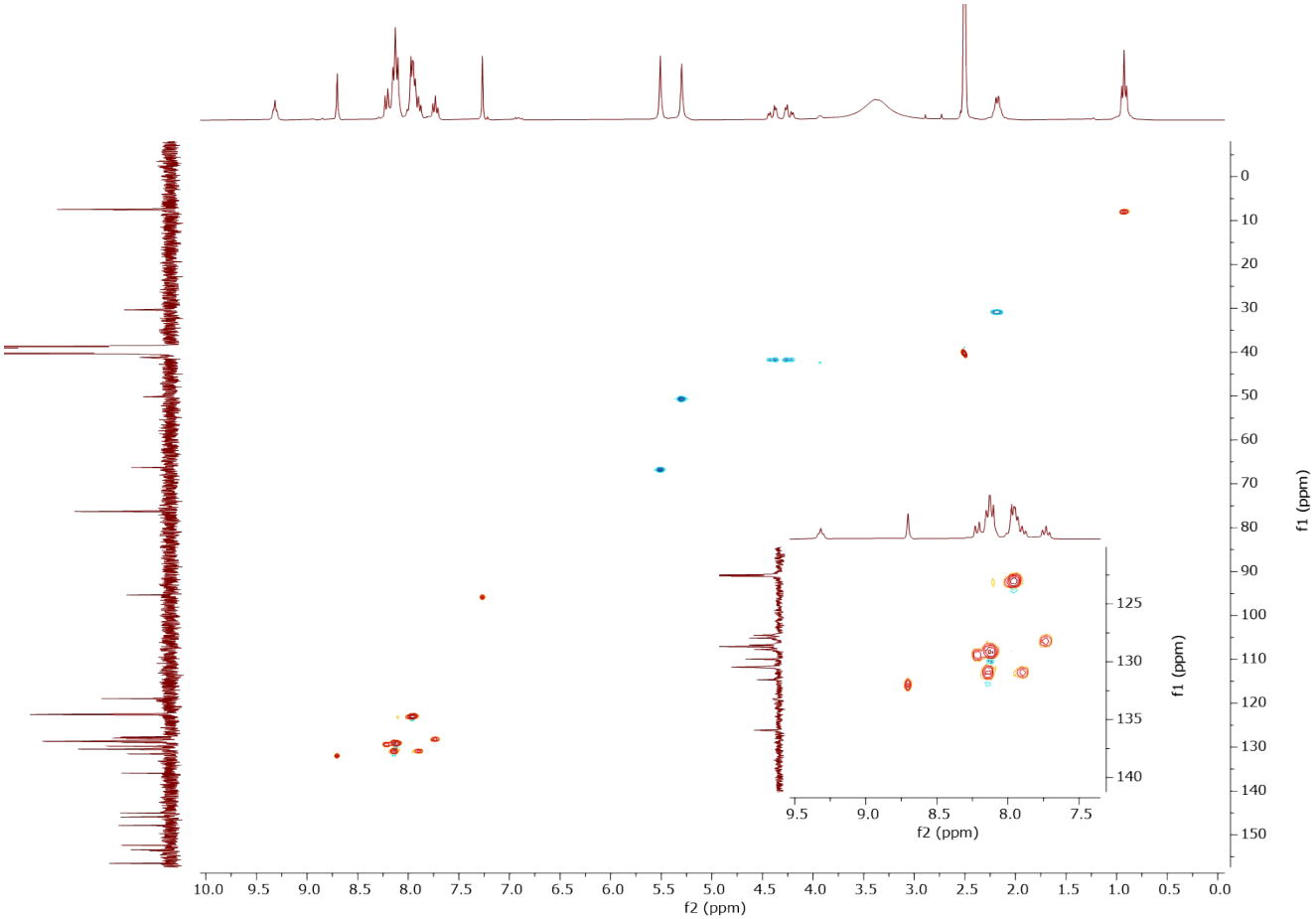

Fig. S6. 2D-HSQC spectrum of CAABE compound. In this 2D spectrum, the red peaks denote CH_3 or CH signals, while the blue spots designate CH_2 signals.

3.2.5. High Resolution Mass Spectrometry (HRMS)

HRMS (ESI+, *m/z*) $[M+H]^+$ calcd for $C_{58}H_{45}N_8O_{12}$ 1045.3157; found 1045.3199.

Elemental Composition Report **Page 1**

Single Mass Analysis
Tolerance = 5.0 PPM / DBE: min = -1.5, max = 100.0
Element prediction: Off
Number of isotope peaks used for i-FIT = 2

Monoisotopic Mass, Even Electron Ions
274 formula(e) evaluated with 6 results within limits (up to 50 closest results for each mass)
Elements Used:
C: 50-60 H: 40-50 N: 0-10 O: 0-12 23Na: 0-1 K: 0-1
Eva R
ERB79_brut_20Oct 715 (3.031) Cm (715:719-753:761) 1: TOF MS ES+ 9.37e+002

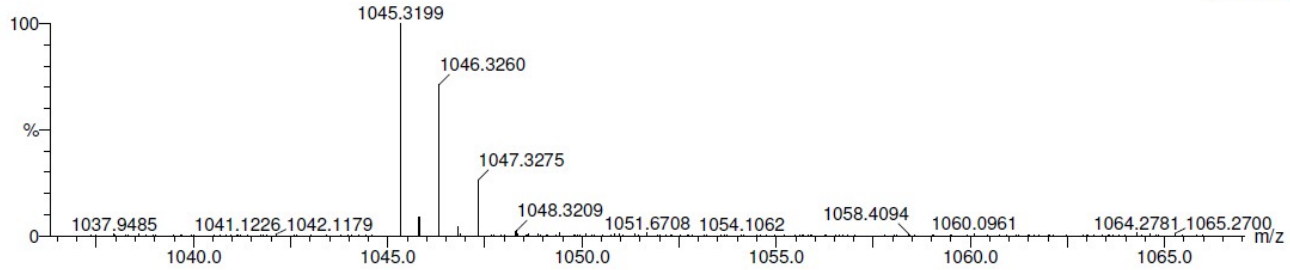

Minimum:				-1.5			
Maximum:		10.0	5.0	100.0			
Mass	Calc. Mass	mDa	PPM	DBE	i-FIT	i-FIT (Norm)	Formula
1045.3199	1045.3188	1.1	1.1	41.5	27.4	1.0	C59 H46 N10 O7 K
	1045.3175	2.4	2.3	36.5	28.1	1.7	C58 H50 N6 O11 K
	1045.3164	3.5	3.3	38.5	28.5	2.1	C57 H47 N10 O7 23Na K
	1045.3157	4.2	4.0	40.5	28.8	2.4	C58 H45 N8 O12
	1045.3245	-4.6	-4.4	37.5	28.3	1.9	C55 H46 N10 O11 23Na
	1045.3247	-4.8	-4.6	32.5	29.2	2.8	C52 H50 N10 O12 K

Fig. S7. HRMS spectrum of the as-synthesized CAABE compound.

3.3. Characterization of CAABE-2

3.3.1 [1]H-NMR Spectra

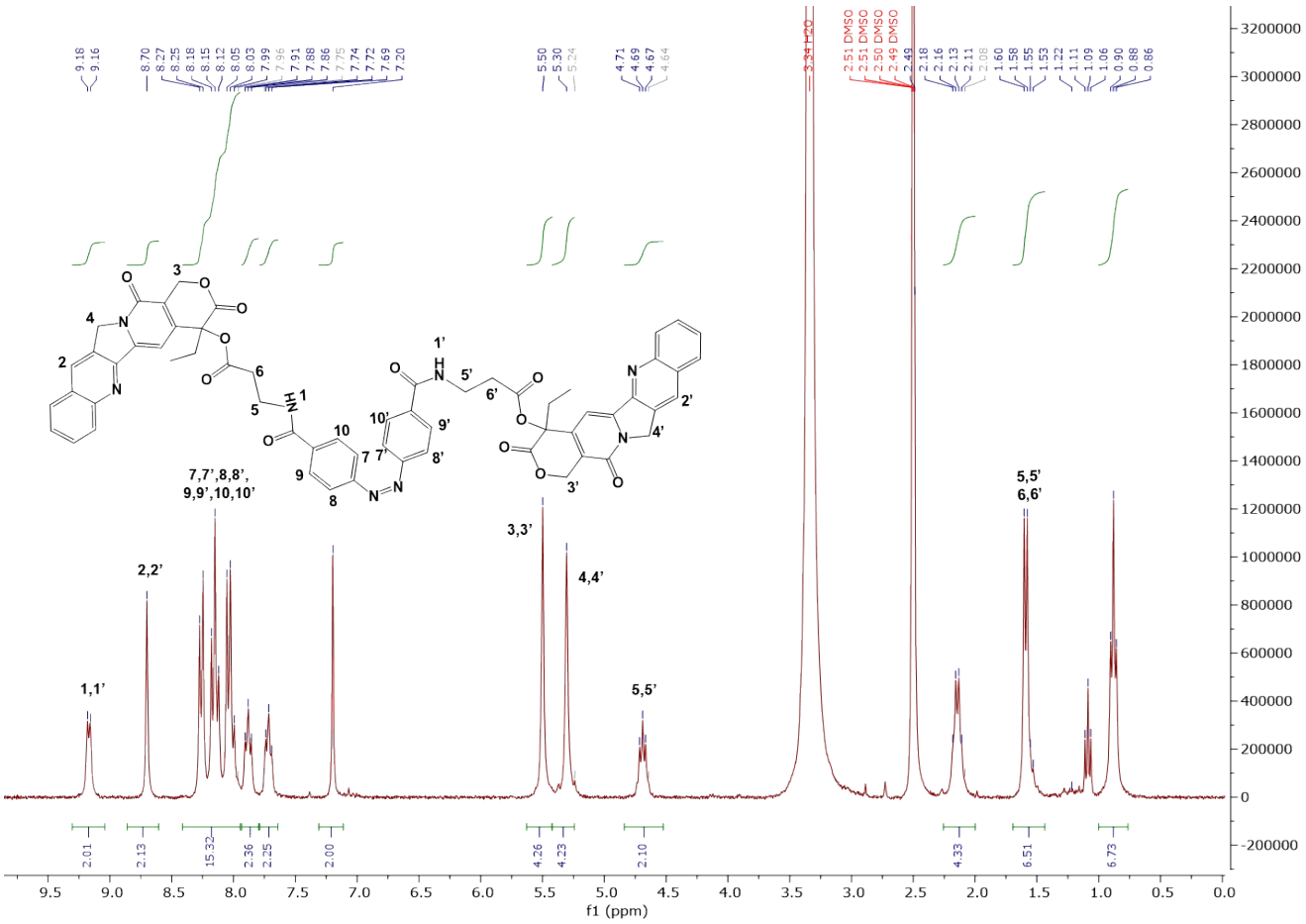

[1]H-NMR (400 MHz, DMSO-d$_6$, δ_H): 0.88 (t, *J*=7.3 Hz, 6H), 1.59 (d, *J*=7.4 Hz, 6H), 2.14 (m, 4H), 4.69 (m, 2H), 5.30 (s, 4H), 5.50 (s, 4H), 7.20 (s, 2H), 7.71 (t, *J*=7.3 Hz, 2H), 7.88 (t, *J*=7.7 Hz, 2H), 8.34 – 7.96 (m, 12H, 4 azo H-meta hydrogen atoms, 4 azo H-ortho hydrogen atoms), 8.70 (s, 2H), 9.17 (d, *J*=6.7 Hz, 2H).

Fig. S8. [1]H-NMR spectrum of CAABE-2 compound.

3.3.2. ^{13}C-NMR Spectra

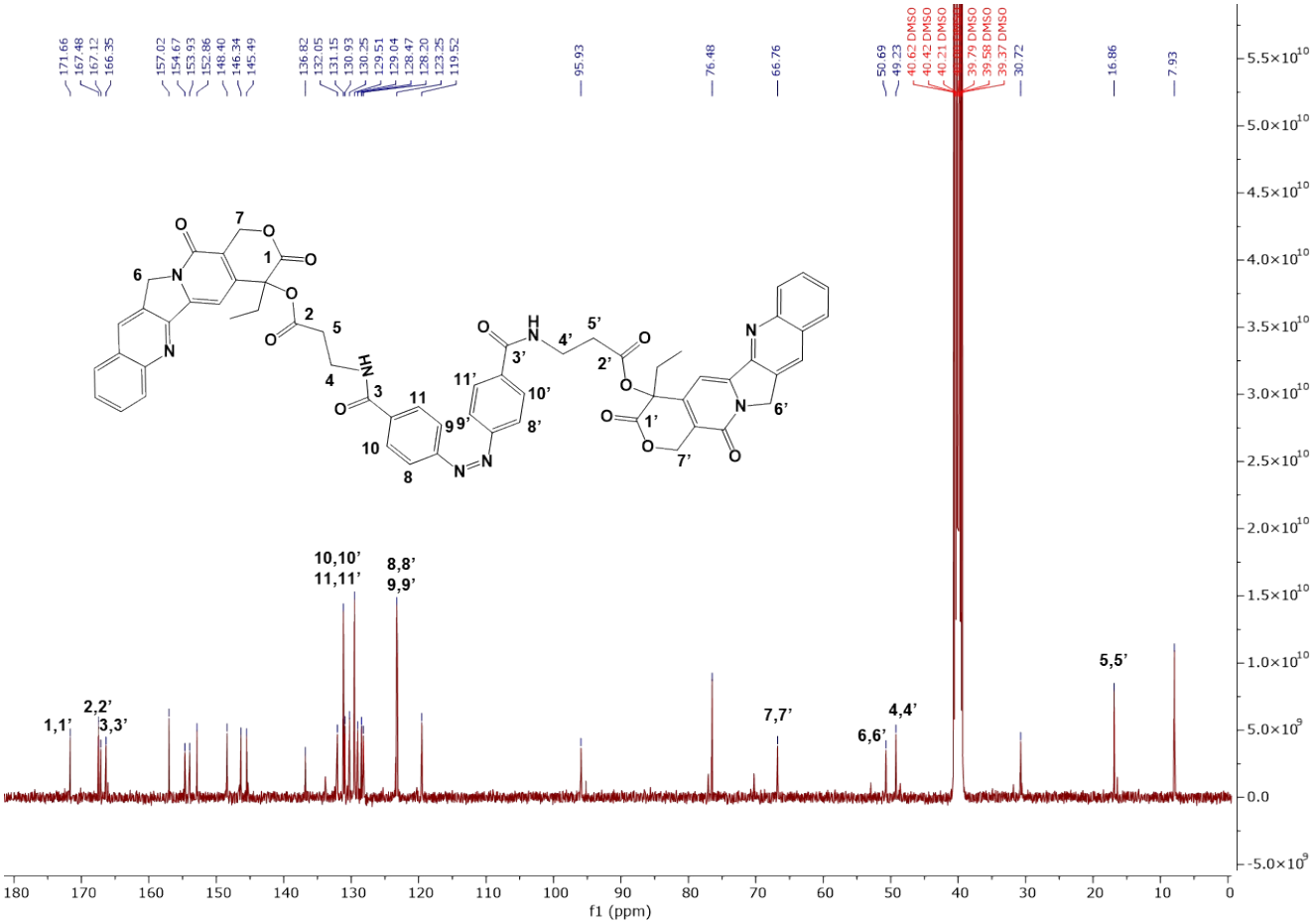

^{13}C-NMR (101 MHz, DMSO-d$_6$, δ_C): 7.93, 16.86, 30.72, 49.23, 50.69, 66.76, 76.48, 95.93, 119.52, 123.25, 128.20, 128.47, 129.04, 129.51, 130.25, 130.93, 131.15, 132.05, 136.82, 145.49, 146.34, 148.40, 152.86, 153.93, 154.67, 157.02, 166.35, 167.12, 167.48, 171.66.

Fig. S9. ^{13}C-NMR spectrum of CAABE-2 compound.

3.3.5. High Resolution Mass Spectrometry (HRMS)

HRMS (ESI+, *m/z*) $[M-H]^+$ calcd for $C_{60}H_{49}N_8O_{12}$, 1073.3470; found 1073.3480.

Elemental Composition Report **Page 1**

Single Mass Analysis
Tolerance = 5.0 PPM / DBE: min = -1.5, max = 100.0
Element prediction: Off
Number of isotope peaks used for i-FIT = 2

Monoisotopic Mass, Even Electron Ions
1360 formula(e) evaluated with 2 results within limits (up to 50 closest results for each mass)
Elements Used:
C: 0-60 H: 0-50 N: 0-8 O: 0-15 Na: 0-3 39K: 0-1
ZORBAX
ERB-571_PRECIPITADO_ CONC 637 (4.904) Cm (634:637-595:598)

1: TOF MS ES+
3.16e+002

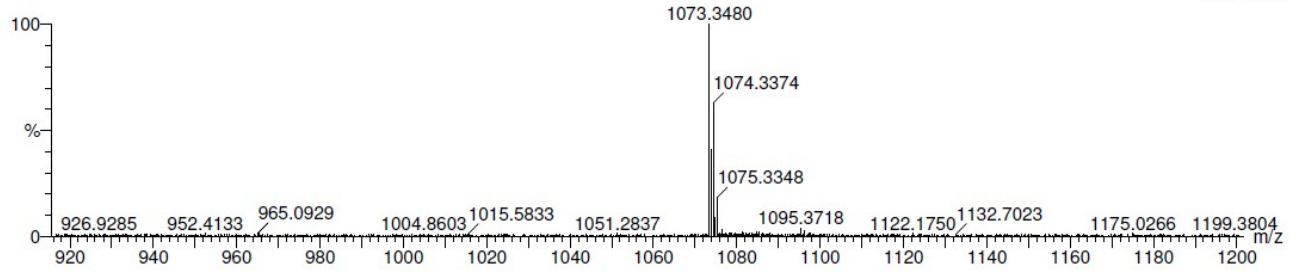

Minimum:				-1.5							
Maximum:		10.0	5.0	100.0							
Mass	Calc. Mass	mDa	PPM	DBE	i-FIT	i-FIT (Norm)	Formula				
1073.3480	1073.3470	1.0	0.9	40.5	34.2	1.0	C60	H49	N8	O12	
	1073.3446	3.4	3.2	37.5	33.6	0.5	C58	H50	N8	O12	Na

Fig. S10. HRMS spectrum of the as-synthesized CAABE-2 compound.

3.3. Photoisomerization of CAABE

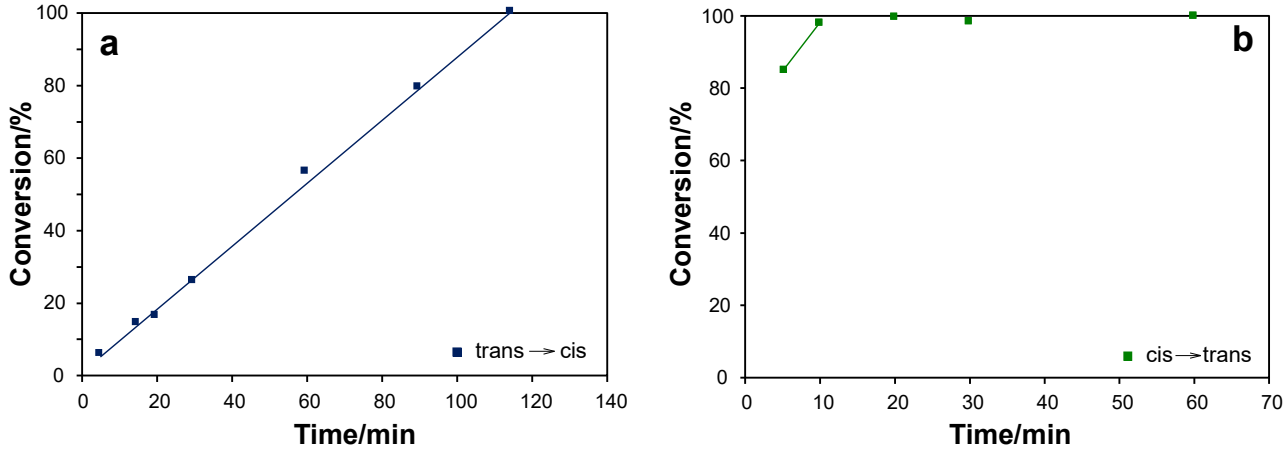

Fig. S11. Plots of conversion percent of *cis/trans*-CAABE isomers as a function of irradiation time (350 nm, *trans*→*cis* ; 450 nm, *cis*→*trans*).

4. Characterization of LSN materials

Nanoparticle morphology was investigated by transmission electron microscopy (TEM) in a Philips CM-10 microscope operating at 100 kV. Particle average diameter was calculated as the media with standard deviation of at least 150 measured nanoparticles. The size distribution of the synthetized nanoparticles in aqueous dispersions was determined using a Zetasizer Nano ZS (Malvern Instruments Ltd., Worcestershire, United Kingdom). For this, solutions of dried materials in deionized water at a concentration of 5 μg/mL were prepared and dynamic light scattering (DLS) measurements were performed at 25 ºC and 173º scattering angle. Liquid nitrogen adsorption isotherms were measured in a Micromeritics ASAP 2420 System apparatus. The pore size distribution was calculated according to the BJH algorithm. Surface area calculations were carried out using the BET method. Finally, residual carbon content in template-extracted materials was monitored by elemental analysis (FISONS, EA 1108 CHNS-O).

4.1. Nitrogen adsorption-desorption isotherms (BET-BJH)

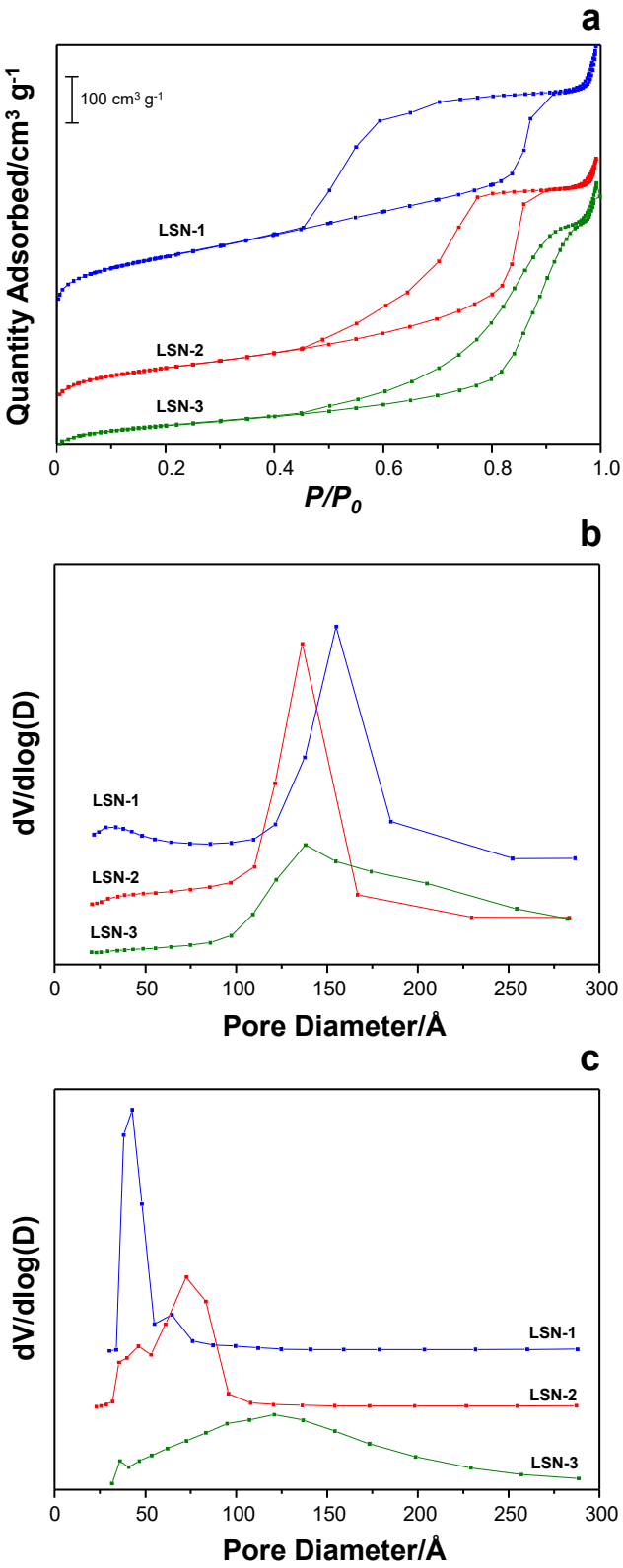

Fig. S12. Nitrogen sorption isotherms (a), cavity sizes distribution (b), and pore entrance sizes distribution (c) of as-synthesized materials.

4.2. Particle size distribution (DLS)

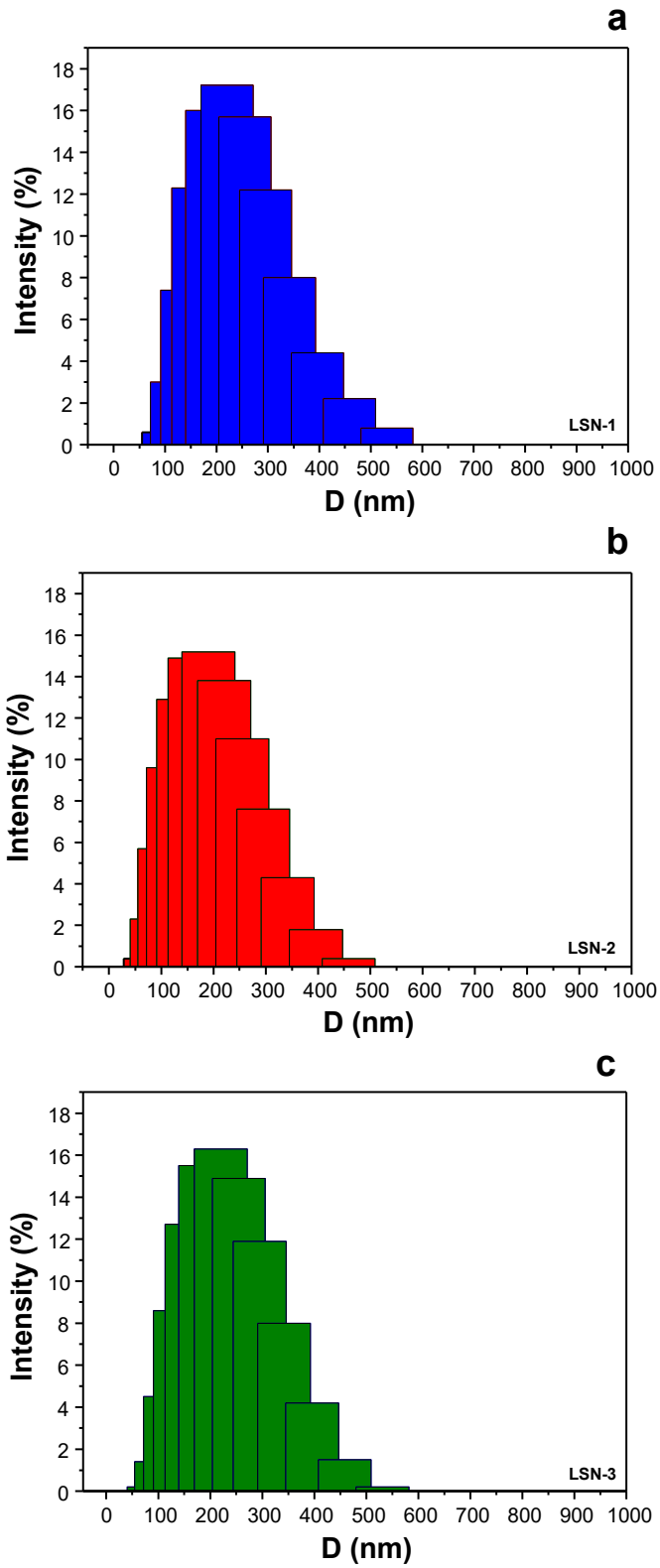

Fig. S13. Particle hydrodynamic diameter of as-synthesized materials as determined in water by DLS (intensity output).

5. STORM

5.1. Slide Preparation and STORM Imaging

Samples were prepared and imaged via STORM using a modified version of a previously published protocol.[8] Particles were resuspended in 500 µL phosphate-buffered saline (PBS, pH 7.4), briefly sonicated, and the resulting solution was added to a 35 mm MatTek glass slide with a 14 mm sample well. Particles were allowed to settle to the bottom of the glass slide for approximately 3-4 minutes.

During this time, fresh imaging buffer was prepared according to the protocol recommended by the microscope manufacturer (Nikon). The imaging buffer consisted of Tris buffer (690 µL, 50 mM Tris-HCl (pH 8.0), 10 mM NaCl, 10 % glucose), a GLOX solution (7 µL, glucose-oxidase (14 mg), catalase (17 mg/mL), 10 mM Tris-HCl (pH 8.0), 50 mM NaCl), and 2-mercaptoethanol (7 µL). Excess PBS was removed from the glass slide, sufficient imaging buffer was added to cover the well, and the sample was immediately imaged on a Nikon Eclipse Ti-E microscope.

The sample was excited using a 405 nm laser and a minimum of 7,500 frames were collected for each run. All molecules with a minimum peak height greater than 300 were considered for further analysis in NIS-Elements.

5.2. Data Analysis and Reconstruction

Several regions of interest (ROIs) were created to isolate data specific to individual spheres, from which Cartesian coordinates of the detected molecules were extracted to .txt files for data reconstruction.

The extracted Cartesian coordinates for each particle were used in a custom least-squares sphere of best fit algorithm written in Python, producing the calculated radius and center of sphere. This was done by minimizing the function:[9]

$$J = \sqrt{\frac{1}{I}\sum_{i=1}^{I}\left((x_i - x_c)^2 + (y_i - y_c)^2 + (z_i - z_c)^2 - r_c^2\right)^2} \qquad (SE3)$$

I = number of data points

(x_i, y_i, z_i) = i^{th} measurement of the origin

(x_c, y_c, z_c) = center of sphere

r_c = radius of sphere

$$\begin{bmatrix} x_c \\ y_c \\ z_c \end{bmatrix} = \frac{1}{2}\begin{bmatrix} \sum_i x_i(x_i-\bar{x}) & \sum_i x_i(y_i-\bar{y}) & \sum_i x_i(z_i-\bar{z}) \\ \sum_i y_i(x_i-\bar{x}) & \sum_i y_i(y_i-\bar{y}) & \sum_i y_i(z_i-\bar{z}) \\ \sum_i z_i(x_i-\bar{x}) & \sum_i z_i(y_i-\bar{y}) & \sum_i z_i(z_i-\bar{z}) \end{bmatrix}^{-1}\begin{bmatrix} \sum_i \left(x_i^2+y_i^2+z_i^2\right)(x_i-\bar{x}) \\ \sum_i \left(x_i^2+y_i^2+z_i^2\right)(y_i-\bar{y}) \\ \sum_i \left(x_i^2+y_i^2+z_i^2\right)(z_i-\bar{z}) \end{bmatrix} \quad (SE4)$$

$$r_c = \sqrt{\frac{1}{I}\sum_{i=1}^{I}((x_i-x_c)^2+(y_i-y_c)^2+(z_i-z_c)^2)} \quad (SE5)$$

For ease of calculation, the sphere of best fit along with the Cartesian coordinates were transposed to reflect the center of the sphere as the origin. Distances of each detected molecule from the center of the sphere were determined by the Pythagorean Theorem, again written in Python:

$$d = \sqrt{(x_i-x_c)^2+(y_i-y_c)^2+(z_i-z_c)^2} \quad (SE6)$$

d = distance from origin to data point (nm)

(x_i, y_i, z_i) = Cartesian coordinates of individual data points

(x_c, y_c, z_c) = center of sphere

Penetration depths of each molecule into the sphere were determined by calculating the difference between the distance of each molecule from the sphere center and the calculated radius of the sphere. Averaging the penetration depths for each respective sphere yielded the mean penetration depth. The total number of molecules within a sphere was found by counting the number of Cartesian coordinates detected by STORM.

Using the transformed Cartesian coordinates of each molecule and the sphere of best fit, a 3D model of each sphere was reconstructed using Blender modeling software. A Python code was written to import the molecule coordinates and construct a wire-frame sphere to reflect what was imaged via STORM. Movies showing a full 360° view of each sphere were exported as .mp4 files, as described below:

Data	Isomer	movie
Mathematica plot	*cis*-CAABE	Video SV8 cis-loading movie.mp4
Fluorescence STORM overlay movie	*trans*-CAABE	Video SV9 cis-sphere movie.mp4
Mathematica plot	*cis*-CAABE	Video SV10 trans-loading movie.mp4
Fluorescence STORM overlay movie	*trans*-CAABE	Video SV11 trans-sphere movie.mp4

6. Controlled release by photoisomerization

RP-HPLC was carried out in an Agilent HPLC LC1220 Infinity System equipped with an autosampler and fluorescence detector 1260 Infinity (for multiple wavelength detection) was used. HPLC method used a C18 reverse phase column (MEDITERRANEA SEA18, 5 µm, 25 × 0.46 mm, Teknokroma, Sant Cugat del Vallés, Spain). The products were eluted with an isocratic flow (0.8 mL min^{-1}) of CH_3CN/H_2O-CF_3COOH pH 4.5 60:40 (v/v). 20 µL of standards and resulting solutions were injected.

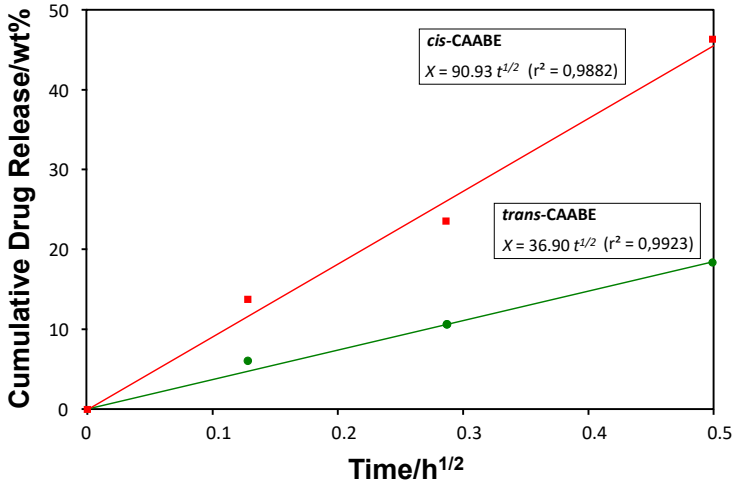

Fig. S14. Plots of Higuchi's kinetic model for the release of *cis/trans*-CAABE from LSN-1 nanoparticles after photoisomerization with UV-Visible light in water, at 37 ºC.

7. Biological validation

7.1. Description of the hand-crafted irradiation camera

An irradiation camera emitting at 350 nm was prepared for the *in vitro* photoisomerization experiments. This contains a plate with 21 LEDs of 3.2 V, 75 mA and 0.24 W. The maximum illumination energy was 2000 mCd, corresponding to 2.2 mW cm^{-2}. The control unit was made by two microprocessors working in arduino system and a selector allowed to modulate irradiation power from 1 to 100%. The photoexcitation area was fitted to dimensions of a 96-well cell culture plate. Additional images of this device are presented in Video SV-1.

7.2. Biological activity of CAABE molecule

CAABE and CPT cytotocixity over HeLa cells was determined using the MTS (3-(4,5-dimethylthiazol-2-yl)-5-(3-carboxymethoxyphenyl)-2-(4-sulfophenyl)-2H-tetrazolium) colorimetric assay. Cells were seeded in 96-well plate at a density of 4500 (HeLa). Then, cells were treated with CPT or an equivalent amount of CAABE, with final doses ranging from 2.5 to 0.0005 µg mL−1 during 72 h. At the end of the incubation period, 15 µL of MTS solution was added into each well and incubated for another 4 h. Absorbance was measured with a Perkin Elmer Wallac 1420 VICTOR2 Multilabel HTS Counter (Northwolk, CT, USA) at the wavelength of 490 nm. IC50 survival data were calculated by non-linear regression sigmoidal dose-response (variable slope) curve-fitting using Prism 6.0 software (GraphPad, San Diego, CA, USA). Three independent experiments (n=3) were performed for every sample and each experiment was carried out by in triplicate. The results are shown in Fig. S15 and Table S1.

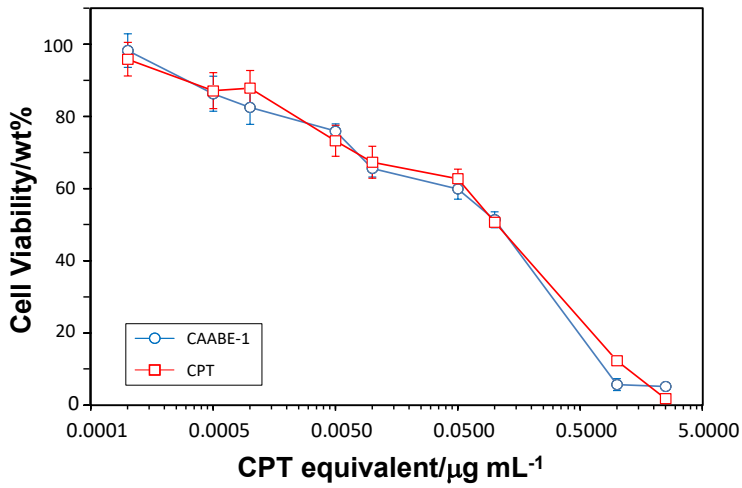

Fig. S15. MTS cell viability assay of CPT and CAABE in HeLa cell line. Cell viability data are expressed as mean ± SEM (n=3).

Table 2. IC_{50} values of CPT and CAABE over HeLa cell line calculated from data in Fig. S15.[a]

Input	CPT	CAABE
IC_{50}	0.05478 ± 0.0205	0.04138 ± 0.0175

[a] Each value indicates the mean ± SEM. Experiments were carried out in triplicate. CPT or CPT equivalent are expressed in μg mL^{-1}.

7.3. Biocompatibility study of LSN-1 material

The potential cytotocixity of LSN-1 material on HeLa cells was determined using the MTS (3-(4,5-dimethylthiazol-2-yl)-5-(3-carboxymethoxyphenyl)-2-(4-sulfophenyl)-2H-tetrazolium) colorimetric assay. Cells were seeded in 96-well plate at a density of 4500 (HeLa) or 8000 (U251, SH-SY5Y) cells per well and incubated in 5% CO_2 at 37 °C for 24h. Then, cells were treated with the CAABE-free LSN-1 nanoparticles, with final doses ranging from 100 to 0.005 μg mL−1 during 72 h. At the end of the incubation period, 15 μL of MTS solution was added into each well and incubated for another 4 h. Absorbance was measured with a Perkin Elmer Wallac 1420 VICTOR2 Multilabel HTS Counter (Northwolk, CT, USA) at the wavelength of 490 nm. Three independent experiments (*n*=3) were performed for every sample and each experiment was carried out by in triplicate. The results are shown in Fig. S16.

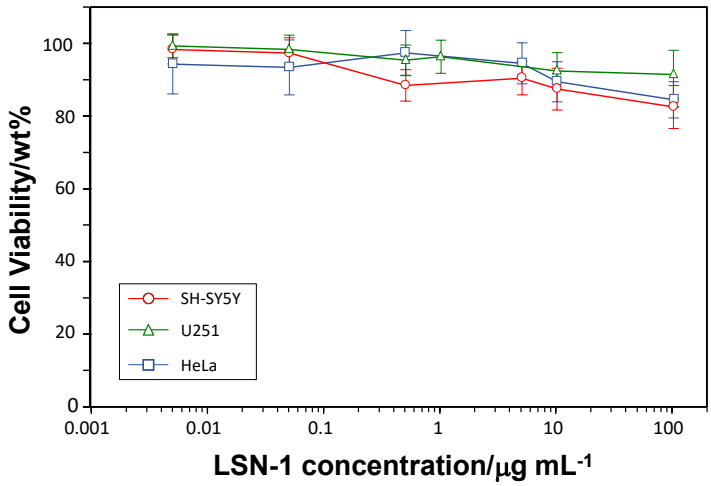

Fig. S16. MTS cell viability assay of LSN-1 material in SH-SY5Y, U251 and HeLa cell lines. Cell viability data are expressed as mean ± SEM (*n*=3).

7.4. Biological activity of CAABE/LSN-1 nanoparticles before light irradiation

In order to discard any cytotocixity of CAABE-loaded LSN-1 material on SH-SY5Y, U251, and HeLa cells during the 24 h incubation previous to UV-light irradiation, we carried out a series of experiments by using the 3-(4,5-dimethylthiazol-2-yl)-5-(3-carboxymethoxyphenyl)-2-(4-sulfophenyl)-2H-tetrazolium (MTS) colorimetric assay. Cells were seeded in 96-well plate at a density of 4500 (HeLa) or 8000 (U251, SH-SY5Y)

cells per well and incubated in 5% CO_2 at 37 °C for 24h. Then, cells were treated for 24 h with the CAABE-loaded LSN-1 nanoparticles (5% wt/wt prodrug contents), with final CAABE dose ranging from 0.48 to 0.0005 μg mL^{-1}. At the end of the incubation period, 15 μL of MTS solution was added into each well and incubated for another 4 h. Absorbance was measured with a Perkin Elmer Wallac 1420 VICTOR2 Multilabel HTS Counter (Northwolk, CT, USA) at the wavelength of 490 nm. Three independent experiments (*n*=3) were performed for every sample and each experiment was carried out in biological triplicate. The results are shown in Fig. S17.

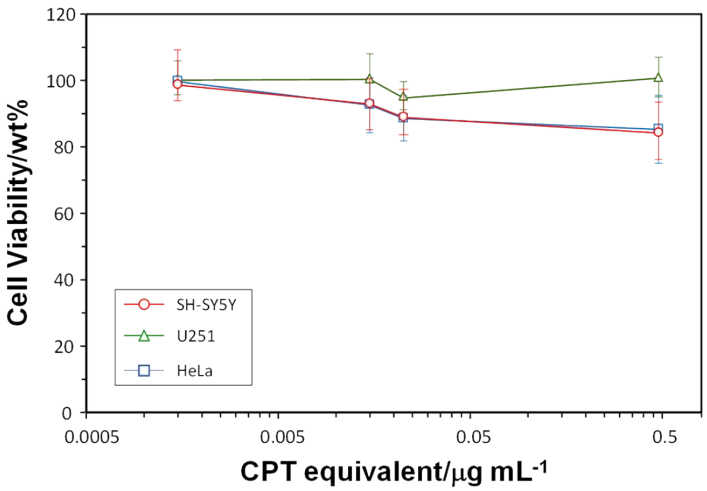

Fig. S17. MTS cell viability assay of CAABE-loaded LSN-1 material in SH-SY5Y, U251, and HeLa cell lines during the 24 h incubation previous to UV-light irradiation. Cell viability data are expressed as mean SEM (*n*=3).

8. References

1 Z. Tian, J. Wen and J. Ma, *Mol. Simul.*, 2015, **41**, 28–42.

2 M. Böckmann, S. Braun, N. L. Doltsinis and D. Marx, *J. Chem. Phys.*, 2013, **139**, 084108.

3 R. Denschlag, W. J. Schreier, B. Rieff, T. E. Schrader, F. O. Koller, L. Moroder, W. Zinth and P. Tavan, *Phys. Chem. Chem. Phys.*, 2010, **12**, 6204–6218.

4 T. Oie, G. M. Maggiora, R. E. Christoffersen$ and D. J. Duchamp, *Int. J. Quantum Chem.*, 1981, **20**, 1–47.

5 S. Bureekaew, S. Amirjalayer, M. Tafipolsky, C. Spickermann, T. K. Roy and R. Schmid, *Phys. Status Solidi Basic Res.*, 2013, **250**, 1128–1141.

6 G. Sastre, J. Van Den Bergh, F. Kapteijn, D. Denysenko and D. Volkmer, *Dalt. Trans.*, 2014, **43**, 9612–9619.

7 W. Smith and T. R. Forester, *J. Mol. Graph.*, 1996, **14**, 136–141.

8 A. M. Clemments, P. Botella and C. C. Landry, *J. Am. Chem. Soc.*, 2017, **139**, 3978–3981.

9 C. Jennins, A.L., Black, J., Allen, *Shock Vib.*, 2013, **20**, 503–517.